INTERNATIONAL JOURNAL FOR NUMERICAL METHODS IN FLUIDS, VOL. 13, 939–953 (1991)

FINITE ELEMENT METHOD FOR SHALLOW WATER EQUATION INCLUDING OPEN BOUNDARY CONDITION

TOSHIO KODAMA, TOMOYUKI KAWASAKI AND MUTSUTO KAWAHARA
Department of Civil Engineering, Chuo University, 1-13-27 Kasuga, Bunkyo-ku, Tokyo 112, Japan

SUMMARY

A method to deal with an open boundary condition in the analysis of water surface waves, the tide, etc. by means of the finite element method is proposed in this paper. The present method has two important features relating to the treatment of the open boundary condition. The first feature is to consider the non-reflective virtual boundary condition which has been developed in the numerical wave analysis method. The incident wave conditions without spurious reflected waves can be imposed at the open boundary. The second feature is to identify the amplitude of the components of incident waves in terms of observed water elevations in the field of standing waves. This can be done as a parameter identification based on an optimization problem by applying the conjugate gradient method. The applicability of this method to wave propagation problems is verified by several numerical computations.

KEY WORDS Finite element method Shallow water equation Open boundary condition Parameter identification Tokyo Bay

1. INTRODUCTION

In the analysis of surface wave problems such as the tide by numerical methods, e.g. the finite element method and/or the finite difference method, an analytical domain is surrounded by both a land boundary and an artificial boundary which is often called the 'open boundary' and is located artificially offshore. Generally, the perfectly reflective condition is imposed at the land boundary and either the periodic water elevation or velocity is given at the open boundary in the conventional analysis. These conditions have been employed in a number of tidal analyses.[1-3] In the analysis of the tide an unsteady analysis is usually performed because the tide is itself periodic with constant currents from the inflow of rivers, the influence of seasonal winds and residual flow. In this case it is rather incorrect to impose either the periodic water elevation or velocity at the open boundary. The reasons for this are the following. If the amplitude of an observed value such as the tide level is given at the open boundary, progressive waves are generated and propagate towards the land boundary and reflect at this boundary because the initial conditions of water elevation and velocity are assumed to be zero. Then the reflected wave propagates towards the open boundary where it overlaps with the incident wave which is still entering from the open boundary. If the reflected wave is not able to pass through the open boundary to the outer side, the field of standing waves cannot be computed. The amplitude imposed at the location of the open boundary cannot be the same as that of the initial value. The reflected wave reflects at the open boundary and contaminates the solution because the amplitude is necessarily specified at the open boundary in the conventional analysis. There are some cases where these reflected waves can be negligibly small. However, it is impossible to perfectly eliminate the reflected wave, so that

0271–2091/91/180939–15$07.50 *Received November 1989*

numerical techniques are required for the open boundary treatment. To overcome this problem, Tanimoto and Kobune[4] have applied a non-reflective virtual boundary condition at the open boundary in the finite difference method. The reflected waves, which are essentially unknown, can be obtained by computing the difference between the computed values and the incident wave at a few distances inside the open boundary in this method. The procedure of computation is successfully advanced for use in the finite element method in this paper.[5,6]

Conventionally the analysis was performed on the assumption that the incident waves are known. However, it is difficult to estimate the incident wave which corresponds to the actual field data of the water surface wave or the tide. The incident wave can be obtained using spectral analysis of the surface wave field. In the analysis of the tide the incident wave is usually unknown because the tidal wave cannot be separated into incident and reflected components. It is extremely important to divide the tidal wave into incident and reflected components in order to predict the behaviour of the tide. The reflected wave continually changes its configuration but the incident wave is always unchanged. Thus, for example, for the design of a harbour or the prediction of tidal waves the incident wave should be imposed as the boundary condition because the reflected wave must be computed according to the change of configuration of the land boundary. A method to identify the incident wave component is shown in this paper. The amplitude, wave direction, period and phase lag must be known in order to identify the incident wave. The amplitude is dealt with as an unknown factor since the other factors can be easily determined in the case of tide analysis. In the method presented in this paper the identification of the amplitude of incident waves is carried out on the basis of the minimization of residuals between the computed water elevations and observed data recorded at fixed points in the flow field. This can be treated as an optimization problem employing the least squares method. The Fletcher–Reeves method,[7] which is one of the conjugate gradient methods, is used to minimize the performance function. The formulation of this procedure is shown. The validity of this method of estimation is illustrated through several numerical examples.

2. THE BASIC EQUATIONS

A schematic diagram of the analytical domain is shown in Figure 1. The semi-infinite flow region Ω is divided into two parts, i.e. the inner, Ω_1, and outer Ω_O, domains, by the so-called open boundary Γ_O, which is an artificial boundary. The boundary Γ_L is the land boundary. The boundary Γ_∞ is the boundary located at infinity. Here and henceforth, equations are expressed

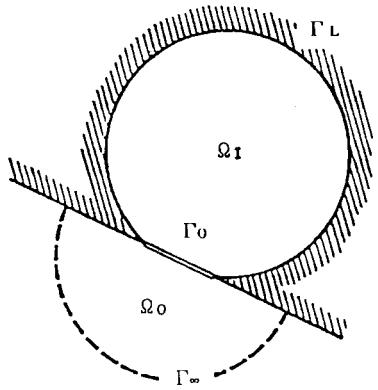

Figure 1. Definition sketch of analytical domain

in indicial notation using co-ordinates X_i $(i=1, 2)$ and time t, and a standard summation convention with repeated indices.

The linearized shallow water equations are employed in this paper because the purpose of this study is restricted to knowing how to deal with the open boundary condition. The equations of motion and continuity are written in the form

$$\frac{\partial u_i}{\partial t}+g\eta_{,i}=0 \quad \text{in } \Omega, \tag{1}$$

$$\frac{\partial \eta}{\partial t}+hu_{i,i}=0 \quad \text{in } \Omega, \tag{2}$$

where u_i and η denote the mean velocity and water elevation respectively and h and g are the sea depth and gravitational acceleration respectively. The following two types of boundary conditions are considered. On the boundary Γ_L the velocity is assumed to be known:

$$u_i=\hat{u}_i \quad \text{on } \Gamma_L, \tag{3}$$

where the 'hat' denotes a prescribed value on the boundary. The non-reflective incident wave conditions, which will be explained in detail in the next section, are imposed at the boundary Γ_O:

$$u_i=\bar{u}_i \quad \text{on } \Gamma_O, \tag{4}$$

$$\eta=\bar{\eta} \quad \text{on } \Gamma_O, \tag{5}$$

where the 'overbar' indicates a prescribed value by the procedure of the present method.

3. TREATMENT OF OPEN BOUNDARY CONDITION

The method to deal with the open boundary condition, which was originally applied by Tanimoto and Kobune[4] to the finite difference method, is successfully advanced for use in the finite element method. The procedures of computation of this method are shown in this section.

The incident wave condition is given on the open boundary to initiate the calculation in the analysis of the tide. It is incorrect to impose the water elevation and velocity as equal to those of only the incident wave, because there exist not only incident waves but also outgoing waves across the open boundary owing to reflection from the inner island and coastline. Such outgoing waves should be freely transmitted through the open boundary. Along the open boundary the co-ordinate n–s is located, of which n is normal to the boundary. The situation of incident waves with an amplitude a_I and a directional angle α_I together with reflected waves is shown in Figure 2. The velocity component in the n-direction and the water elevation can be expressed as the sum of incident (I) and reflected (R) components:

$$\bar{u}_n(n_0, t)=u_n^I(n_0, t)+u_n^R(n_0, t), \tag{6}$$

$$\bar{\eta}(n_0, t)=\eta^I(n_0, t)+\eta^R(n_0, t). \tag{7}$$

It is natural to assume that u_n^I and η^I are known variables:

$$u_n^I(n_0, t)=\frac{g}{c}a_I\cos\alpha_I\sin(k_n n_0+k_s s_0-\omega t-\kappa), \tag{8}$$

$$\eta^I(n_0, t)=a_I\sin(k_n n_0+k_s s_0-\omega t-\kappa), \tag{9}$$

where k_n and k_s are the components of the wave number, ω is the angular frequency, κ is the phase lag and $c=\sqrt{(gh)}$ denotes the wave velocity.

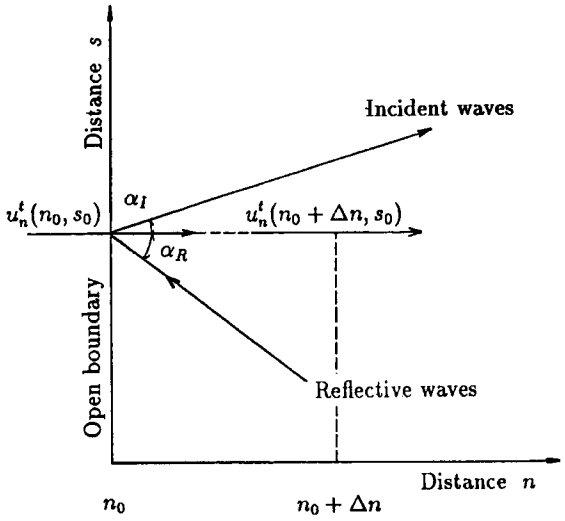

Figure 2. Open boundary

The procedures of computation for the non-reflective boundary condition are shown by the following equations. The components of the reflected wave can be obtained as

$$\Delta u_n = u_n^t(n_0+\Delta n, s_0) - \frac{g}{c} a_I \cos\alpha_I \sin[k_n(n_0+\Delta n)+k_s s_0-\omega t-\kappa], \tag{10}$$

$$\bar{u}_n^{t+\Delta t} = \frac{g}{c} a^I \cos\alpha_I \sin[k_n n_0+k_s s_0-\omega(t+\Delta t)-\kappa]+\Delta u_n \tag{11}$$

for the velocity and

$$\Delta\eta = \eta^t(n_0+\Delta n, s_0) - a_I \sin[k_n(n_0+\Delta n)+k_s s_0-\omega t-\kappa], \tag{12}$$

$$\bar{\eta}^{t+\Delta t} = a_I \sin[k_n n_0+k_s s_0-\omega(t+\Delta t)-\kappa]+\Delta\eta \tag{13}$$

and for the water elevation, where Δu_n and $\Delta\eta$ are the components of the reflected wave at a position Δn inside the open boundary. These components represent the differences between the computed standing wave and the incident wave. If the product of the wave velocity c and time increment Δt equals the distance Δn, this reflected wave will propagate to the open boundary at the next time step. Applying these procedures, incident wave conditions without spurious reflection as expressed by equations (11) and (13) can be imposed at the open boundary. The velocity in the s-direction can be obtained by a similar procedure to that for equations (10) and (11).

4. FINITE ELEMENT METHOD

The weighted residual equations are obtained by applying the conventional Galerkin method to the governing equations. The finite element equations can be described in the following form using the linear interpolation function based on the three-point triangular finite element:

$$M_{\alpha\beta}\dot{u}_{\beta i} + H_{\alpha i\beta}\eta_\beta = 0, \tag{14}$$

$$M_{\alpha\beta}\dot{\eta}_\beta + I_{\alpha i\beta}u_{\beta i} = 0, \tag{15}$$

where the 'overdot' means differentiation with respect to time and $u_{\beta i}$ and η_β denote the velocity at the βth node of the finite element in the ith direction and water elevation at the βth node respectively. The coefficient matrices are

$$M_{\alpha\beta}=\int_{\Omega_I}(\Phi_\alpha\Phi_\beta)\,d\Omega, \qquad H_{\alpha i\beta}=g\int_{\Omega_I}(\Phi_{\alpha,i}\,\Phi_\beta)\,d\Omega, \qquad I_{\alpha i\beta}=h\int_{\Omega_I}(\Phi_{\alpha,i}\,\Phi_\beta)\,d\Omega,$$

in which Φ is the interpolation function for both velocity and water elevation. The two-step explicit finite element method[8] is used for equations (14) and (15) to discretize the time function, which can be derived as follows:

$$\bar{M}_{\alpha\beta}u_{\beta i}^{n+1/2}=\tilde{M}_{\alpha\beta}u_{\beta i}^{n}-\frac{\Delta t}{2}H_{\alpha i\beta}\eta_\beta^n, \tag{16}$$

$$\bar{M}_{\alpha\beta}\eta_\beta^{n+1/2}=\tilde{M}_{\alpha\beta}\eta_\beta^{n}-\frac{\Delta t}{2}I_{\alpha i\beta}u_{\beta i}^n, \tag{17}$$

$$\bar{M}_{\alpha\beta}u_{\beta i}^{n+1}=\tilde{M}_{\alpha\beta}u_{\beta i}^{n}-\Delta t H_{\alpha i\beta}\eta_\beta^{n+1/2}, \tag{18}$$

$$\bar{M}_{\alpha\beta}\eta_\beta^{n+1}=\tilde{M}_{\alpha\beta}\eta_\beta^{n}-\Delta t I_{\alpha i\beta}u_{\beta i}^{n+1/2}. \tag{19}$$

In equations (16)–(19), $\bar{M}_{\alpha\beta}$ denotes the lumped coefficient of $M_{\alpha\beta}$ and $\tilde{M}_{\alpha\beta}$ is the mixed coefficient, which is

$$\tilde{M}_{\alpha\beta}=e\bar{M}_{\alpha\beta}+(1-e)M_{\alpha\beta}, \tag{20}$$

where e is referred to as the lumping parameter.

5. ESTIMATION OF INCIDENT WAVE COMPONENT

The calculation in the previous section can be carried out on the assumption that all information about the incident waves is known. A physical quantity which can be easily observed is the tide elevation at various stations located along coastline. Therefore the incident wave component has to be estimated from the observed values. In this paper a method to estimate the incident wave component is also proposed. In this method the identification of the incident wave component is carried out on the basis of tide levels which are observed at arbitrary points in the flow field. The computational procedures of the estimation are shown in the section.

The incident wave consists essentially of period, wave direction, phase lag and amplitude. In the usual analysis it is justifiable to consider the period, wave direction and phase lag as known constants. Accordingly, only the amplitude of incident waves is identified in this paper. In general, the tidal wave consists of a sum of harmonic waves; hence the amplitudes are expressed in the form

$$a_\lambda^{\mathrm{T}}=\{a_1^{\mathrm{I}}, a_2^{\mathrm{I}}, a_3^{\mathrm{I}}, \ldots, a_n^{\mathrm{I}}\}, \tag{21}$$

where I denotes the incident wave component, λ is the number of wave, n is the total number of waves and T denotes transposition. The observed water elevations at arbitrary points are given as

$$\tilde{\eta}_\mu(t)^{\mathrm{T}}=\{\tilde{\eta}_1(t), \tilde{\eta}_2(t), \tilde{\eta}_3(t), \ldots, \tilde{\eta}_m(t)\}, \tag{22}$$

where 'overtilde' denotes an observed value, μ is the number of an observation point, m is the total number of observation points and t denotes time. The water elevations to be computed at observation points 1–m are expressed as

$$\eta_\mu(a_\lambda, t)^{\mathrm{T}}=\{\eta_1(a_\lambda, t), \eta_2(a_\lambda, t), \eta_3(a_\lambda, t), \ldots, \eta_m(a_\lambda, t)\}. \tag{23}$$

The performance function expressed by the sum of squared residuals between the observed and computed values is assumed to estimate the amplitude on incident waves:

$$J(a_\lambda)=\frac{1}{2}\int_{t_0}^{t_f}[\tilde{\eta}_\mu(t)-\eta_\mu(a_\lambda,t)]^{\mathrm{T}}[\tilde{\eta}_\mu(t)-\eta_\mu(a_\lambda,t)]\,\mathrm{d}t. \tag{24}$$

Since J is a function of amplitude a_λ, optimization of a_λ is then equivalent to minimizing the least squares criterion (24). In estimating the amplitude a_λ, the number of observation points, m must be greater than the number of incident waves, n.

The Fletcher–Reeves method,[7] which is one of the conjugate gradient methods, is successfully applied to the minimization of equation (24). This method is widely employed as an optimal control technique in many engineering fields. The features of this method are that the computational algorithm is relatively simple and only small-size memories are required in the computation. The computational algorithm can be described as follows.

1. Asssume initial amplitude a_λ^0; set allowable constant ε and $k=0$.
2. Compute $\eta_\mu^0(a_\lambda^0,t)$, $J(a_\lambda^0)$ and $\partial\eta_\mu/\partial a_\lambda$.
3. Compute $\partial J(a_\lambda^0)/\partial a_\lambda$ and set $d_\lambda^0=-\partial J(a_\lambda^0)/\partial a_\lambda$.
4. Determine α_λ^k which minimizes $J(a_\lambda^k+\alpha_\lambda^k d_\lambda^k)$.
5. Compute $a_\lambda^{k+1}=a_\lambda^k+\alpha_\lambda^k d_\lambda^k$.
6. Compute $\eta_\mu^{k+1}(a_\lambda^{k+1},t)$ and $J(a_\lambda^{k+1})$.
7. If $|J(a_\lambda^{k+1})-J(a_\lambda^k)|<\varepsilon$, then stop.
8. Compute $\partial J(a_\lambda^{k+1})/\partial a_\lambda$.
9. Compute β_λ^k.
10. Compute $d_\lambda^{k+1}=-\partial J(a_\lambda^{k+1})/\partial a_\lambda+\beta_\lambda^k d_\lambda^k$.
11. Set $k=k+1$ and go to step 4.

Here k is the iteration number and ε is a small number which expresses the convergence allowance. The flowchart is shown in Figure 3.

The sensitivity matrix $\partial\eta_\mu(t)/\partial a_\lambda$ can be obtained by solving the equations

$$\bar{M}_{\alpha\beta}\left(\frac{\partial u_{\beta i}}{\partial a_\lambda}\right)^{n+1/2}=\tilde{M}_{\alpha\beta}\left(\frac{\partial u_{\beta i}}{\partial a_\lambda}\right)^{n}-\frac{\Delta t}{2}H_{\alpha\beta}\left(\frac{\partial \eta_\beta}{\partial a_\lambda}\right)^{n}, \tag{25}$$

$$\bar{M}_{\alpha\beta}\left(\frac{\partial \eta_\beta}{\partial a_\lambda}\right)^{n+1/2}=\tilde{M}_{\alpha\beta}\left(\frac{\partial \eta_\beta}{\partial a_\lambda}\right)^{n}-\frac{\Delta t}{2}I_{\alpha\beta i}\left(\frac{\partial u_{\beta i}}{\partial a_\lambda}\right)^{n}, \tag{26}$$

$$\bar{M}_{\alpha\beta}\left(\frac{\partial u_{\beta i}}{\partial a_\lambda}\right)^{n+1}=\tilde{M}_{\alpha\beta}\left(\frac{\partial u_{\beta i}}{\partial a_\lambda}\right)^{n}-\Delta t H_{\alpha\beta}\left(\frac{\partial \eta_\beta}{\partial a_\lambda}\right)^{n+1/2}, \tag{27}$$

$$\bar{M}_{\alpha\beta}\left(\frac{\partial \eta_\beta}{\partial a_\lambda}\right)^{n+1}=\tilde{M}_{\alpha\beta}\left(\frac{\partial \eta_\beta}{\partial a_\lambda}\right)^{n}-\Delta t\, I_{\alpha\beta i}\left(\frac{\partial u_{\beta i}}{\partial a_\lambda}\right)^{n+1/2}, \tag{28}$$

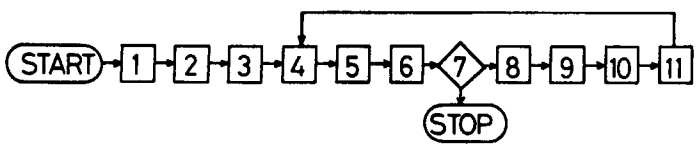

Figure 3. Computational algorithm for identification

subjected to the boundary conditions

$$u_n^{\mathrm{I}}(n_0, t)=\frac{g}{c}\cos\alpha_{\mathrm{I}}\sin(k_n n_0+k_s s_0-\omega t-\kappa), \tag{29}$$

$$\eta^{\mathrm{I}}(n_0, t)=\sin(k_n n_0+k_s s_0-\omega t-\kappa). \tag{30}$$

These equations can be easily obtained by differentiating the incident boundary conditions in equations (8) and (9). The step length α_λ^k is obtained by solving the equation

$$\frac{\partial J}{\partial \alpha_\lambda}=-\int_{t_0}^{t_{\mathrm{f}}}\left(\frac{\partial \eta_\mu}{\partial d_\lambda}d_\lambda\right)^{\mathrm{T}}[\tilde{\eta}_\mu-\eta_\mu(a_\lambda, t)]\,\mathrm{d}t+\alpha_\gamma\int_{t_0}^{t_{\mathrm{f}}}\left(\frac{\partial \eta_\mu}{\partial d_\lambda}d_\lambda\right)^{\mathrm{T}}\left(\frac{\partial \eta_\mu}{\partial d_\gamma}d_\gamma\right)\mathrm{d}t=0. \tag{31}$$

The gradient β_λ^k can be calculated as

$$\beta_\lambda^k=\frac{[\partial J(a_\lambda^{k+1})/\partial a_\lambda]\,\partial J(a_\lambda^{k+1})/\partial a_\lambda}{[\partial J(a_\lambda^k)/\partial a_\lambda]\,\partial J(a_\lambda^k)/\partial a_\lambda}. \tag{32}$$

6. NUMERICAL EXAMPLES

Two numerical examples are shown to verify the applicability of the present method.

Standing waves in one-dimensional channel

Analyses of standing waves are carried out to compare the results with the analytical solutions. The finite element idealization of a one-dimensional channel with a constant depth of 10 m is shown in Figure 4. The total numbers of nodal points and finite elements are 303 and 400 respectively. On the boundaries AD and BC the normal velocities are assumed to be zero. The perfectly reflective condition is imposed at the boundary CD. The boundary AB is the open boundary at which the non-reflective condition is imposed. Two incident wave conditions as shown in Table I are created.

For the computation the time increment $\Delta t=0{\cdot}005$ s and selective lumping parameter $e=0{\cdot}9$ are employed. Computed results of the water elevation and velocity in each case are illustrated in Figures 5–8. The computed results are compared with the analytical solutions and the results

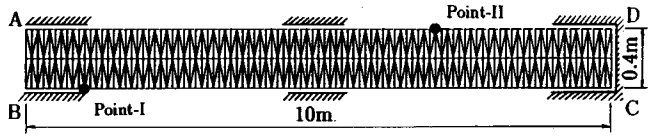

Figure 4. Finite element idealization

Table I. Condition of incident waves

	Amplitude (m)	Angular frequency (rad s^{-1})
Case 1	$a_1=0{\cdot}1,\ a_2=0{\cdot}0$	$\omega_1=6{\cdot}2832$
Case 2	$a_1=0{\cdot}3,\ a_2=0{\cdot}2$	$\omega_1=6{\cdot}2832,\ \omega_2=3{\cdot}1416$

$\eta^{\mathrm{I}}=\sum_{n=1}^{2}a_n\sin(\omega_n t)$.

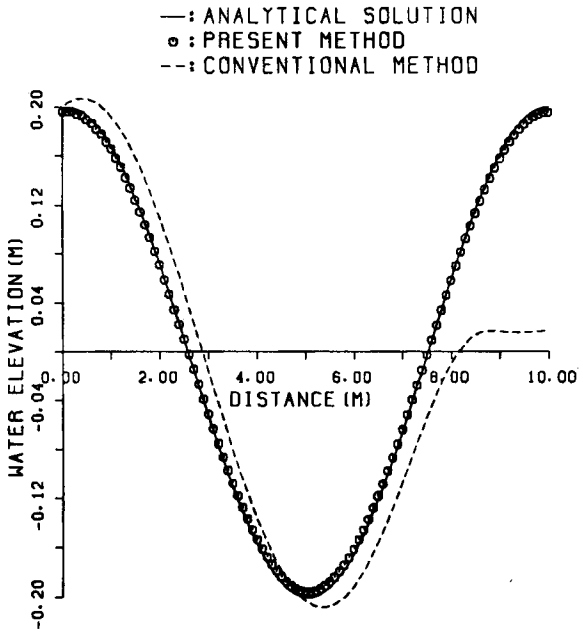

Figure 5. Computed water elevation (Case 1)

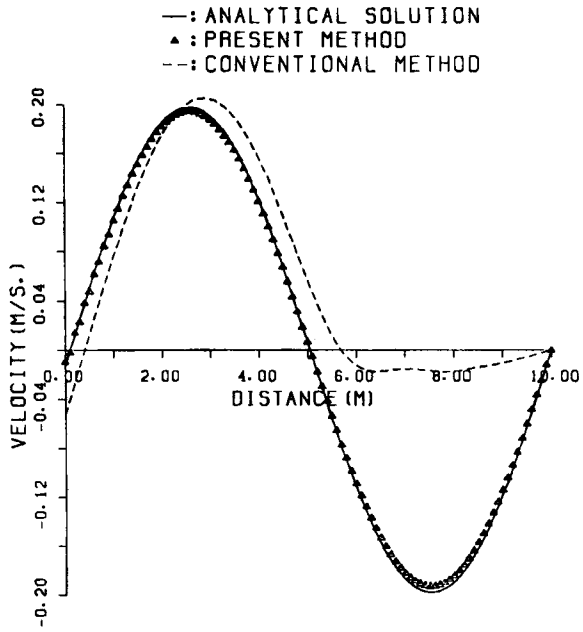

Figure 6. Computed velocity (Case 1)

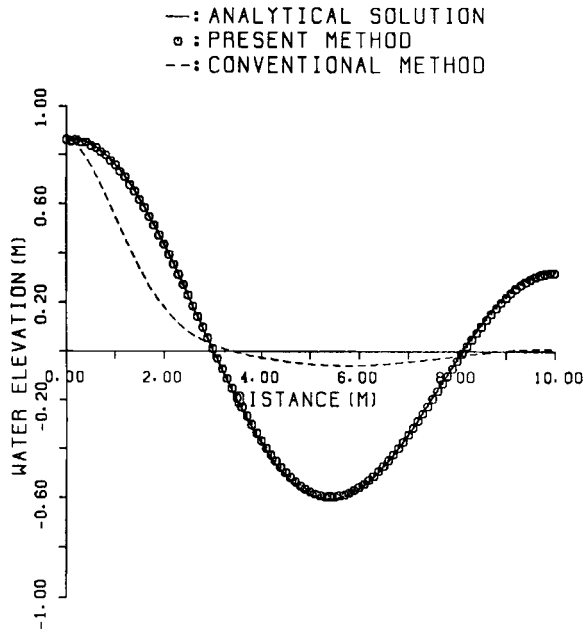

Figure 7. Computed water elevation (Case 2)

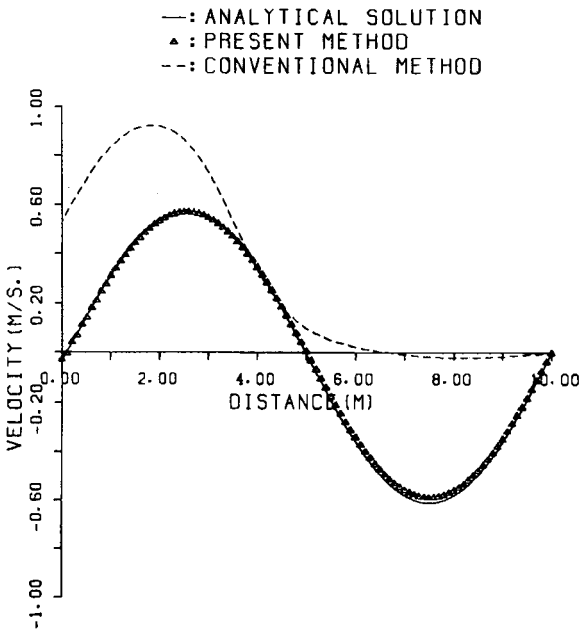

Figure 8. Computed velocity (Case 2)

obtained by the conventional method. Both water elevation and velocity computed by the present method are in good agreement with the analytical solutions.

However, the results by the conventional method do not agree with the analytical solutions. Conventionally, the wave is computed imposing the known function at the open boundary. This result is called that of the conventional method. The final converged steady solution of the conventional method cannot be obtained. From this fact it is seen that the conventional method, which imposes only water elevations at the open boundary, cannot simulate the standing waves.

The identification of the amplitude of the incident wave is performed in the previous two cases. In Figure 4 the full circles are the observation points of the water elevation, which can be chosen arbitrarily. The boundary condition and computational condition are the same as in the previous numerical examples. The observed water elevations which are employed in the inverse analysis have been obtained by the analysis previously performed. In these cases the results which should be identified are shown in Table I. Computed results are described as follows.

Case 1. In this case one wave amplitude is identified employing only one observed value at Point I (see Figure 9). The initial estimated amplitude is assumed to be zero. The transition of the performance function and the stage of convergence are shown in Figures 10 and 11 respectively. The amplitude of the incident waves can be estimated with only one iteration.

Case 2. Two wave amplitudes are estimated in this case. The previous computational results at Points I and II (see Figures 12 and 13) are employed as the observed values. In Figures 14 and 15 the transition of the performance function and the state of convergence respectively are illustrated. Two iteration cycles are required to identify the parameters in this case.

From these results it is seen that if the water elevations obtained by the analysis previously performed are used as the observed values, then the identification of the amplitude can be carried out within a few iteration cycles.

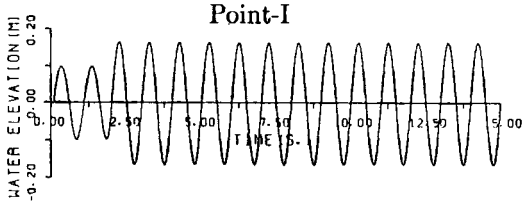

Figure 9. Time variation of water elevation at Point I

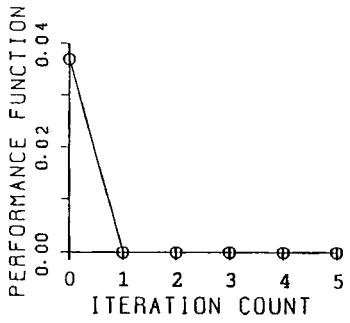

Figure 10. Transition of performance function J

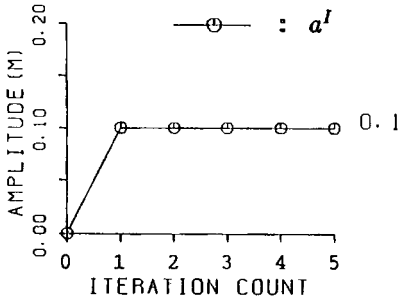

Figure 11. State of convergence of the amplitude

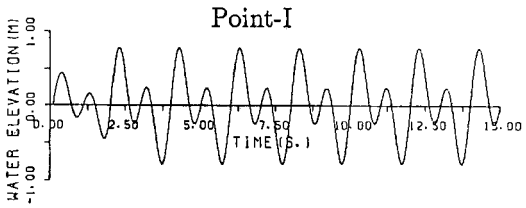

Figure 12. Time variation of water elevation at Point I

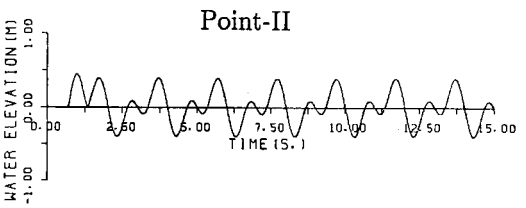

Figure 13. Time variation of water elevation at Point II

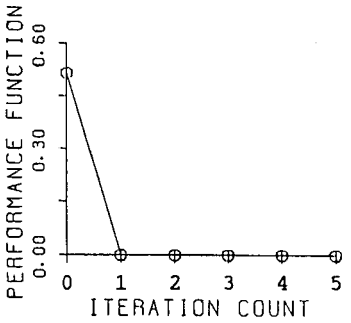

Figure 14. Transition of performance function J

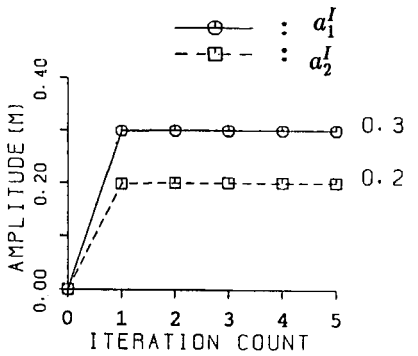

Figure 15. State of convergence of the amplitude

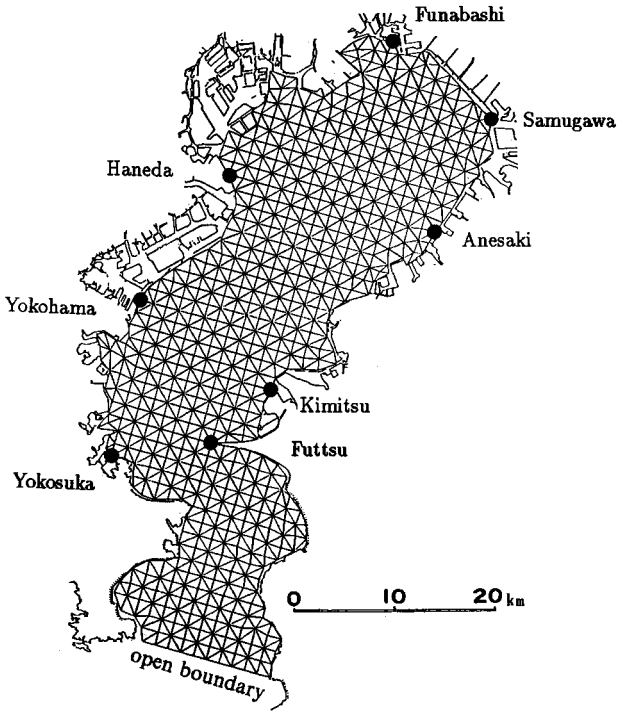

Figure 16. Finite element idealization of Tokyo Bay

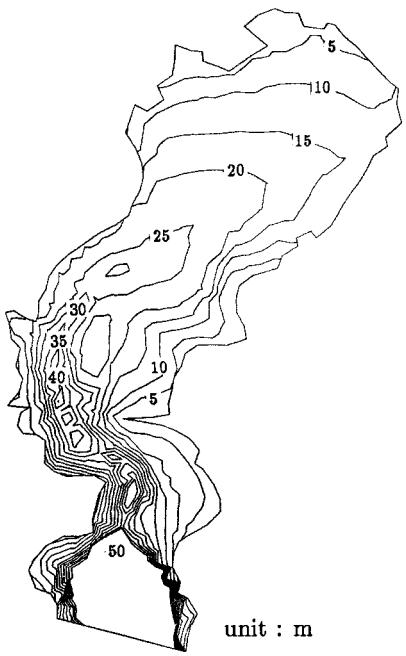

Figure 17. Configuration of water depth

Tide analysis of Tokyo Bay

Simulation of the tide in Tokyo Bay is performed to verify the applicability of the present method in a practical problem. The identification of the amplitude is carried out on the basis of the observed data. The computed water elevations at each observation point and the velocities are compared with the observed values. The finite element idealization is shown in Figure 16. The total numbers of nodes and elements are 685 and 1216 respectively. The city names in this figure indicate the points where the tide gauge records have been observed. The configuration of Tokyo Bay is modelled as shown in Figure 17 with reference to the *Maritime Chart of Tokyo Datum.*[9]

For the boundary condition the perfectly reflective condition is imposed on the land boundary. On the open boundary, four main tidal constituents (M_2, S_2, K_1, O_1) which are shown in Table II are assumed. The amplitudes of these tidal constituents are estimated by the identification method described in Section 5. The treatment of non-reflectivity is carried out on the open boundary. For the computation the time increment $\Delta t = 20$ s and parameter $e = 0{\cdot}9$ are employed.

The variations of tide level given by the *Harmonic Constant Table*[10] at each observation point are illustrated in Figure 20. The identification can be performed under the observed values. The initial estimated values of amplitude are assumed to be zero for all constituents. The transition of the performance function is described in Figure 18 and the state of convergence is illustrated in Figure 19. The four constituents of amplitude can be estimated within about three iteration cycles. The time variations of tide level which are computed under the above estimated amplitude are shown in Figure 20 with the observed tidal levels. The tide levels of the present method are in

Table II. Condition of incident waves

Constituent	Angular frequency (rad h^{-1})	Phase delay (rad)
M_2	$\omega_M = 0{\cdot}5059$	$\kappa_M = -5{\cdot}8398$
S_2	$\omega_S = 0{\cdot}5236$	$\kappa_S = -5{\cdot}6018$
K_1	$\omega_K = 0{\cdot}2626$	$\kappa_K = -1{\cdot}3290$
O_1	$\omega_O = 0{\cdot}2433$	$\kappa_O = -1{\cdot}3211$

$$\eta^I = \sum_{n=1}^{4} a_n \sin(\omega_n t - \kappa_n).$$

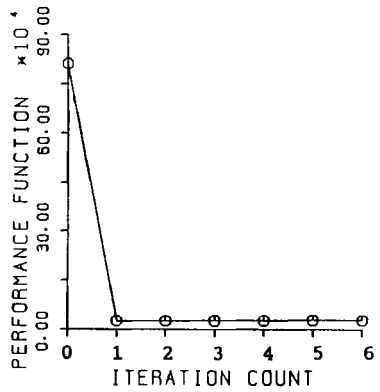

Figure 18. Transition of performance function J

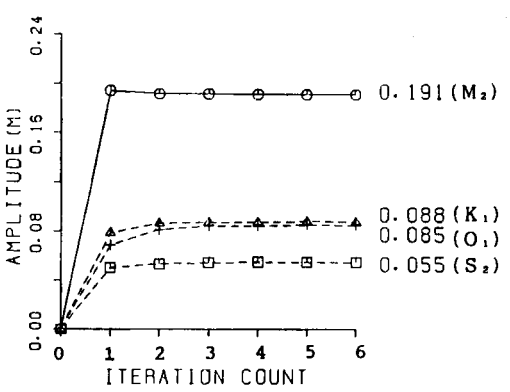

Figure 19. State of convergence of the amplitude

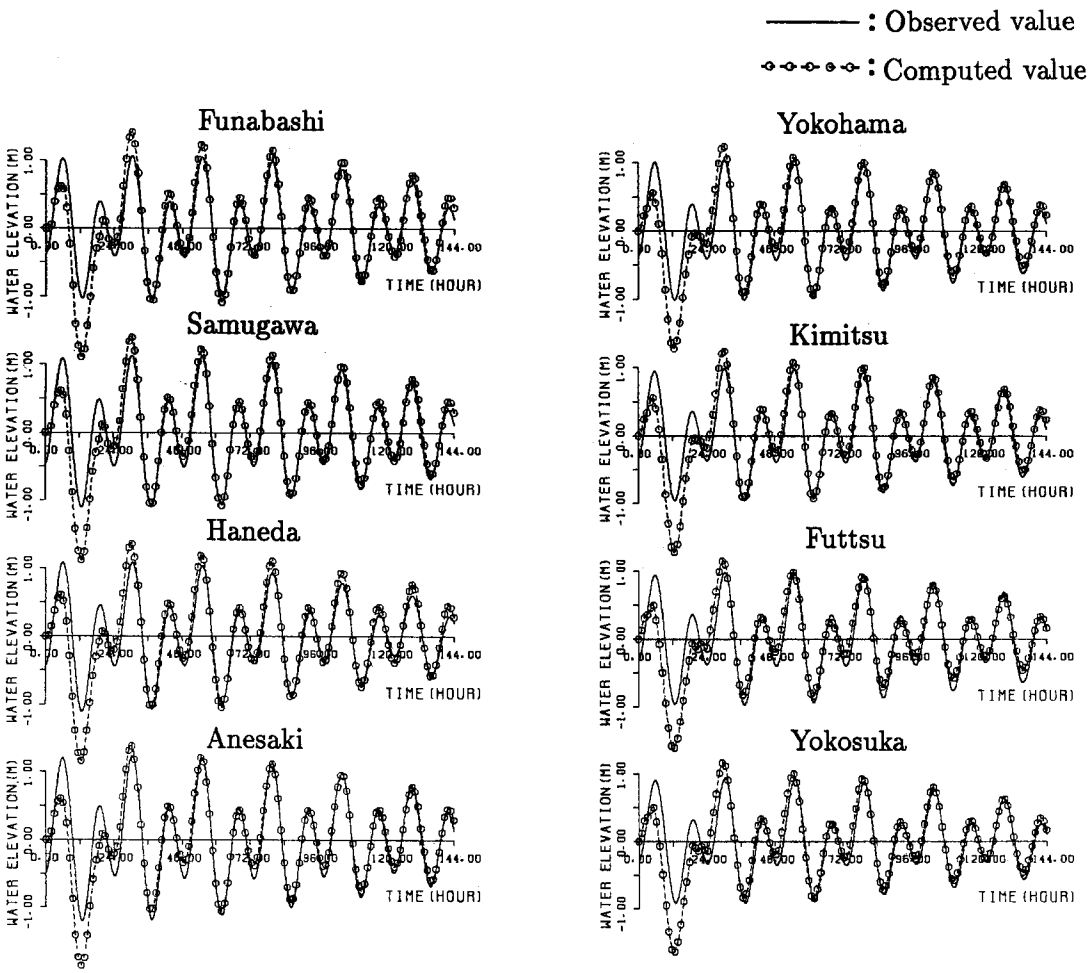

Figure 20. Comparison of time variation of tide level

quite good agreement with the observed data. The maximum water elevations at each observation point in the case of M_2-constituent are shown in Figure 21. The open and full circles denote the computed and observed values[2] respectively. The results of the present method agree well with the observed data. The computed velocities are compared with the measurements in the *Charts of Tidal Stream* of the Maritime Safety Agency[11] in Figure 22. In both the cases of maximum southeast stream and turning time of southeast to northwest the results of the present method agree well with the measurements. From the above results it is seen that the tide level and velocity at arbitrary points in the flow field can be predicted by the present method.

7. CONCLUSIONS

A new method to estimate the amplitude of incident waves in tide analysis has been proposed, including the method to treat an open boundary condition. The main conclusions obtained are as follows.

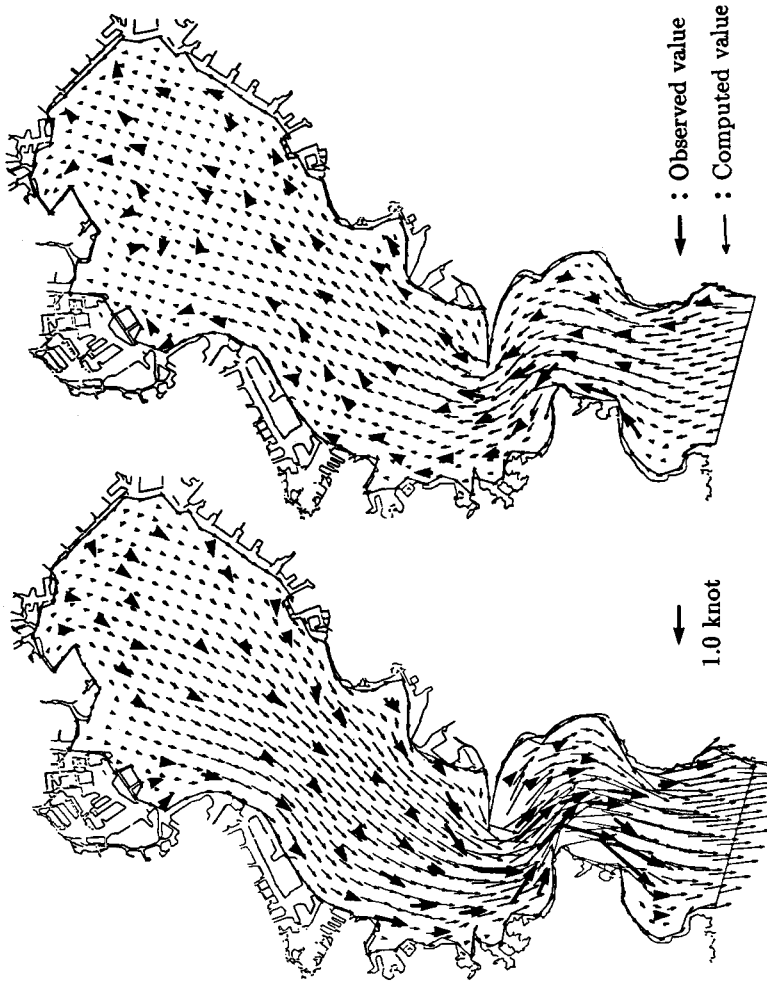

Figure 22. Comparison of velocity

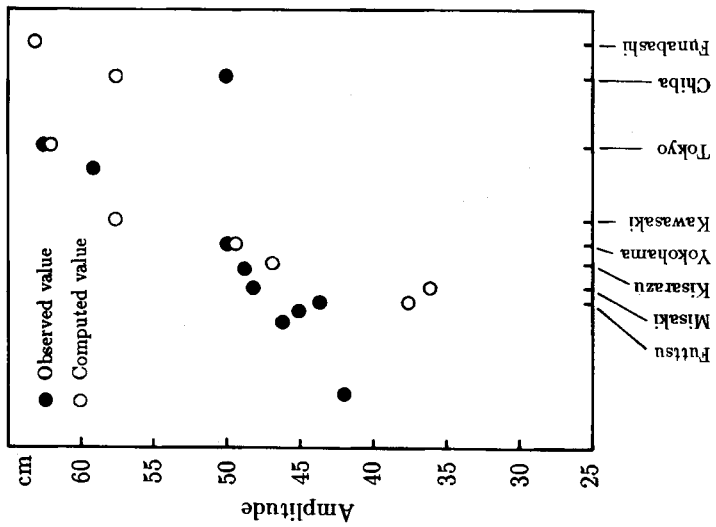

Figure 21. Comparision of maximum amplitude of tide

(1) The method which imposes the non-reflective boundary condition was successfully obtained and applied to the open boundary condition in tide analysis using the finite element method.
(2) The method to identify the incident wave which has to be employed in tide analysis was formulated. The estimation of the amplitude of incident waves can be performed by minimization of the residuals between the computed and observed water elevations.
(3) To show the adaptability of this method, several comparative studies were carried out on the one-dimensional channel model. The results of the present method were in good agreement with the analytical solutions. On the other hand, it was clarified that the standing waves could not be computed by the conventional method.
(4) Applying the estimation technique to numerical examples of the tidal analysis of Tokyo Bay, the identification of wave amplitude could be completely performed within a few iteration cycles, and these estimated parameters give results which are in excellent agreement with the observed data.
(5) Since the tidal wave is divided into incident and reflected waves in the present method, this method can easily be applied to analyse the behaviour of the tide in cases where the analytical domain has different configurations after several modifications of the boundary. This is important for practical applications to predict tidal flow.

From the above conclusions it is seen that the present method is a useful and effective tool for analysing surface wave problems such as the tide. It is straightforward to extend this method not only to linear tidal analysis but also to general water wave problems.

ACKNOWLEDGEMENTS

The numerical computations in this paper were carried out using the FACOM VP-30 computer of Chuo University. Part of this research was supported by Grant in Aid of Science and Engineering, Ministry of Education, No. 01613001.

REFERENCES

1. M. Kawahara, M. Kobayashi and K. Nakata, 'Multiple level finite element analysis and its applications to tidal current flow in Tokyo Bay', *Appl. Math. Modell.*, **17**, 197–211 (1983).
2. T. Horie, 'Hydraulic investigation on seawater flow and substance dispersion in estuarine and coastal regions, *Technical Note of Port & Harbour Research Institute* (*Ministry of Transport*) *No. 360*, 1980 (in Japanese).
3. Y. Kodera, W. Fujiwara and T. Tanaka, 'Forecasting system of water height and tidal current', *Mitsui Zosen Tech. Rev. No. 123*, 1984, pp. 17–23 (in Japanese).
4. K. Tanimoto and K. Kobune, 'Computation of waves in a harbor basin by a numerical wave analysis method', *Proc. 22nd. Japanese Conf. on Coastal Engineering*, JSCE, 1978, pp. 249–253, Tokyo (in Japanese).
5. T. Kodama, N. Kaneko and M. Kawahara, 'A treatment of open boundary condition in shallow water equation', in T. J. Chung *et al.* (eds), *Finite Element Analysis in Fluids*, University of Alabama in Huntsville Press, Huntsville, AL, 1989, pp. 1361–1366.
6. T. Kodama and M. Kawahara, 'A method to treat incident wave condition in shallow water equation', in S. S. Y. Wang (ed.), *Sediment Transport Modelling*, ASCE 1989, New Orleans, pp. 178–183.
7. H. Kanoh, *Theory and Computational Methods in Optimization*, Corona, 1987, Tokyo (in Japanese).
8. M. Kawahara, H. Hirano, K. Tsubota and K. Inagaki, 'Selective lumping finite element method for shallow water flow', *Int. j. numer. methods fluids*, **2**, 89–112 (1982).
9. Maritime Safety Agency, *Maritime Chart of Tokyo Datum No. 90*, 1984 (in Japanese).
10. Maritime Safety Agency, *Harmonic Constant Table*, 1989 (in Japanese).
11. Maritime Safety Agency, *Charts of Tidal Stream in Tokyo Bay, No. 6216*, 1989 (in Japanese).